SHAPE−DEPENDENT ADSORPTION OF SELENIUM AND TELLURIUM BY $M^{II}FE_2O_4$

Weiyi Pan, Weiling Sun

Peking University, College of Environmental Sciences and Engineering, Beijing, China

wypan@pku.edu.cn

Keywords: Selenium; Tellurium; $M^{II}Fe_2O_4$; Adsorption

Introduction

Magnetic materials, such as ferrite ($M^{II}Fe_2O_4$) and magnetite (Fe_2O_3), have been extensively applied to remove oxyanions (eg. SeO_4^{2-}, SeO_3^{2-}, AsO_4^{3-}) because their great adsorption capacity and excellent saturation magnetization (Sun et al., 2004; Sun et al., 2015). Both the size and shape of materials, in particular shape, will determine the availability of certain active facets or low coordinated sites on their surfaces, which can affect the binding between magnetic materials and oxyanions and/or the activity and selectivity of a particular reaction (Zaera 2013). Thus, in addition to the novel properties, the influence of material shapes on the adsorption, catalysis, or energy storage, has become a recent area for research (Zhuang et al., 2015; Zeara 2013). However, how the shapes of $M^{II}Fe_2O_4$ influence its adsorption to oxyanions is far from understood.

In this study, Selenite (SeO_3^{2-}, Se(IV)), selenate (SeO_4^{2-}, Se(VI)), tellurite (TeO_3^{2-}, Te(IV)), and telluric (TeO_4^{2-}, Te(VI)), the main species of Se and Te in wastewater and natural waters, were selected as model oxyanions. $MnFe_2O_4$ and $CoFe_2O_4$ microwire and microsphere, synthesized through hydrothermal methods, were selected as model $M^{II}Fe_2O_4$ materials. The prepared $M^{II}Fe_2O_4$ were characterized using powder X-ray diffraction (XRD), transmission electron microscope (TEM), alternating gradient magnetometer (AGM), automatic titrating, and N_2 adsorption–desorption method. The adsorption behaviors of Se(IV)/Se(VI) and Te(IV)/(VI) by $M^{II}Fe_2O_4$ microwire and microsphere were investigated, and the effect of pH on adsorption were also discussed. The underlying adsorption mechanisms were analyzed using zeta potential, attenuated total reflection flourier transformed infrared spectroscopy (ATR-FTIR), and X-ray photoelectron spectroscopy (XPS) analysis. Density functional theory (DFT), as useful and powerful tool, was employed to explore the adsorption mechanism.

Methods

$M^{II}Fe_2O_4$ microwire were synthesized by adding stoichiometric amounts of Fe^{3+}, Mn^{2+} or Co^{2+} and NaAc and polyethylene glycol were added to 40 mL ethylene glycol with vigorous stirring. For $M^{II}Fe_2O_4$ microsphere, Fe^{3+}, Mn^{2+} or Co^{2+} and nitrilotriacetic acid were added to 40 mL mixed deionized water and isopropyl alcohol with vigorous stirring. All the resulting solutions were heated at 180 °C-200 °C in an oven for 6 h. The products were dried after washed for several times, and calcined.

Results

The TEM images clearly showed the sphere structure of $MnFe_2O_4$ (Mn-S) (Fig. 1a, b) and $CoFe_2O_4$ (Co-S) (Fig. 1c, d) and Fig. 1e-h exhibited porous wires $MnFe_2O_4$ (Mn-W) (Fig. 1e, f) and $CoFe_2O_4$ (Co-S) (Fig. 1g, h). The properties of four types of $MnFe_2O_4$ were shown in Table 1. $M^{II}Fe_2O_4$ exhibited different adsorption behaviors to Se and Te: (1) Microwire (Mn-W and Co-W) adsorbed more Se(IV)/(VI) than microsphere (Mn-S and Co-S), whereas it was contrary for Te(IV)/(VI); (2) Mn-W showed the highest adsorption capacity for Se(IV)/(VI) while Mn-S had highest adsorption capacity for Te(IV)/(VI) among these four types of $MnFe_2O_4$. A decreasing trend was observed for Se(IV)/(VI) and Te(IV)/(VI) adsorption by $M^{II}Fe_2O_4$ with increasing pH.

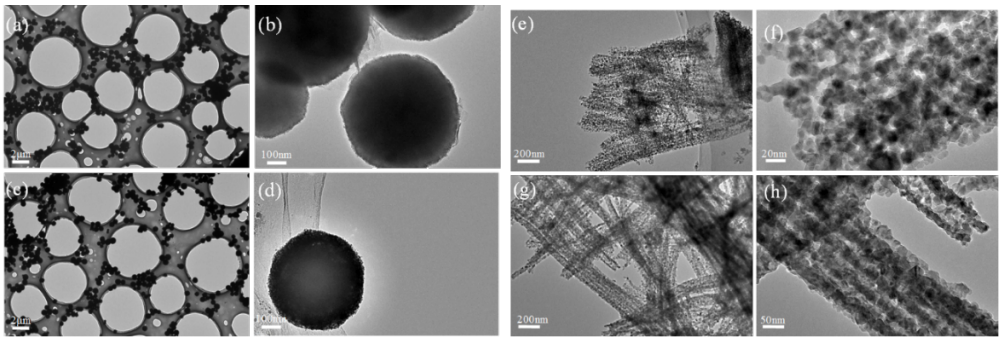

Figure 1. TEM images of Mn-S (a, b), Co-S (c, d) and Mn-W (e, f), Co-W (g, h).

Table 1. Ms, BET surface area and surface hydroxyl amount information.

Sample	BET surface area(m^2/g)	$Q_{surface\text{-}OH}$ (mmol/g)	Magnetization saturation (emu/g)
Co-S	89.5	0.177	91.90
Co-W	16.9	0.289	64.32
Mn-S	92.4	0.162	79.31
Mn-W	35.4	0.342	60.13

The moving of point of zero charge (pH_{pzc}) suggested inner-sphere adsorption might be the predominant mechanism for Se(IV) and Te (IV) adsorption and Se(VI) and Te(VI) adsorption is dominated by outer-sphere (Peak and Sparks 2002). Other experimental and DFT calculation showed the same results.

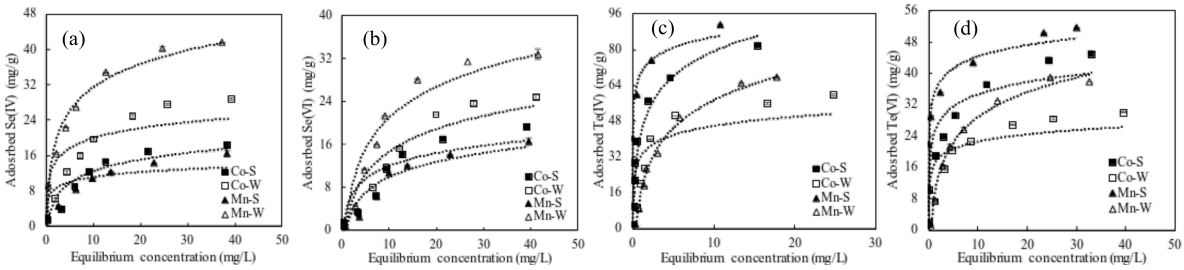

Figure 2. (a) Se(IV), (b) Se(VI), (c) Te(IV) and (b) Te(VI) adsorption by MFe_2O_4 (pH=7±0.5, I=0.05 M NaCl, dash line: Langmuir model fitting results)

Conclusion

This study found microsphere and microwire ferrites exhibited different adsorption behaviors towards Se and Te because of different surface areas and surface –OH amounts. The predominant mechanism for Se(IV) and Te(IV) is inner-sphere adsorption and outer-sphere adsorption for Se(VI) and Te(VI). XPS and ATR-FTIR results and DFT calculation were consistent with experimental results.

References

Peak, D., & Sparks, D. L. (2002). Mechanisms of selenate adsorption on iron oxides and hydroxides. *Environmental science & technology*, 36(7), 1460-1466

Sun, S., Zeng, H., Robinson, D. B., Raoux, S., Rice, P. M., Wang, S. X. Li, G. (2004). Monodisperse MFe_2O_4 (M= Fe, Co, Mn) nanoparticles. *Journal of the American Chemical Society*, 126(1), 273-279

Sun, W., Pan, W., Wang, F., & Xu, N. (2015). Removal of Se (IV) and Se (VI) by MFe_2O_4 nanoparticles from aqueous solution. *Chemical Engineering Journal*, 273, 353-362

Zaera, F. (2013). Nanostructured materials for applications in heterogeneous catalysis. *Chemical Society Reviews*, 42(7), 2746-2762

Zhuang, M., Zheng, Y., Liu, Z., Huang, W., & Hu, X. (2015). Shape-dependent performance of TiO_2 nanocrystals as adsorbents for methyl orange removal. RSC Advances, 5(17), 13200-13207